Heliyon 10 (2024) e26964

Contents lists available at ScienceDirect

Heliyon

journal homepage: www.cell.com/heliyon

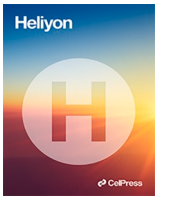

Research article

Revisiting thermo-physical property models of Al_2O_3-Water nanofluid for natural convective flow

Tahmidul Haque Ruvo, Md. Shahneoug Shuvo, Sumon Saha *

Department of Mechanical Engineering, Bangladesh University of Engineering and Technology, Dhaka, 1000, Bangladesh

ARTICLE INFO

Keywords:
Nanofluid
Effective thermal conduction coefficient
Effective absolute viscosity
Nusselt number
Thermal enhancement

ABSTRACT

One of the comprehensive ways of heat transport performance augmentation of thermo-fluid systems is to use nanofluid over base fluid. This study mainly scrutinizes several existing models of thermal conduction coefficient and absolute viscosity of Al_2O_3-water nanofluid with the experimental data. A benchmark problem of natural convective flow is selected to test the performance of the available nanofluid models. The Rayleigh number varies between 10^3 and 10^9, while the solid-volume proportion (φ) changes from 0 to 4%. The governing mathematical model is numerically discretized via the Galerkin finite element procedure under appropriate auxiliary conditions. The results produced by the models are verified with the existing experimental findings based on the evaluation of the Prandtl number and average Nusselt number. It has been confirmed that the AH model (Azmi's viscosity and Ho's conductivity models) is suitable for lower nanoparticle concentration ($\varphi = 0.01$), the AM model (Azmi's viscosity and Maxwell's conductivity models) for moderate concentration ($0.01 < \varphi < 0.04$), and the NH model (Ngueyn's viscosity and Ho's conductivity models) for higher value of the solid-volume proportion ($\varphi = 0.04$).

1. Introduction

Heat transfer augmentation demonstrates the improvement of thermal performance of any heat exchanging media, heat transferring process, heat generating components, and so on. It is presently an essential research and development topic in any thermal management system, energy and power sector, aerospace technologies, heating and cooling of electronic components and electronic devices, thermal energy storage, solar collectors, etc. One of the best techniques for augmentation is raising the thermal conduction coefficient of typical working liquids by adding nano-sized particles of higher thermal conductivity. Choi and Eastman [1] developed the name 'nanofluid' in 1995. They demonstrated that tiny amounts of nanoparticles, sizes between 1 and 100 nm, uniformly dispersed into a typical liquid, e.g., water, ethylene glycol, or oil, could appreciably enhance the heat transport rate. They also argued that the few experimental investigations focused on evaluating nanofluids' thermal conductivity and dynamic viscosity. Mansour et al. [2] examined how different models of nanofluid's properties affected the thermo-hydraulic behavior of pipe flow. Besides, applying Fourier sine transforms to find the exact solution of nanofluids' temperature and velocity profiles opened the door to groundbreaking research in the augmentation of heat transfer performance using nanofluids [3,4].

A significant number of computational and experimental investigations were conducted by several researchers who analyzed the effectivity of nanofluid in the field of fluid flow, energy, and thermal sciences. Kakac and Pramuanjaroenkij [5] reviewed that the

* Corresponding author.
E-mail address: sumonsaha@me.buet.ac.bd (S. Saha).

https://doi.org/10.1016/j.heliyon.2024.e26964
Received 20 October 2023; Received in revised form 15 February 2024; Accepted 22 February 2024
Available online 27 February 2024

Table 1
Thermo-fluid properties of base fluid: water and nanoparticles: Al_2O_3 at 25°C [26].

Properties	Water	Al_2O_3
Dynamic viscosity, μ (Pa.s)	0.001003	–
Thermal conduction coefficient, k ($Wm^{-1}K^{-1}$)	0.613	25
Heat capacitance, C_p ($Jkg^{-1}K^{-1}$)	4179	765
Density, ρ (kgm^{-3})	997.1	3970
Coefficient of volumetric thermal expansion, β (K^{-1})	2.10×10^{-4}	0.85×10^{-5}

thermo-fluid performance of a thermal system improved by convection with nanofluids. They suggested that a significant number of experimental studies and theoretical modeling on effective thermal diffusivity and conductivity were necessary to utilize the full potential of nanofluids for forced convection enhancement. Kasaeian et al. [6] surveyed the effect of nanofluids in porous media and confirmed that the nanofluids enhanced the thermal performance. Pinto and Fiorelli [7] reviewed the investigations of heat transfer enhancement mechanisms where nanofluid was used as a working liquid. Besides, the hydrodynamic properties of nanofluid and the forced convective flow enhancement were reviewed by Hussein et al. [8]. It was summarized that the heat transport performance of nanofluids improved because of the dispersion of nanoparticles, which improved the thermal conduction coefficient of liquids and the chaotic motion of particles, which increased the fluids' turbulence and fluctuation. In another investigation, Ismail et al. [9] reviewed the recent applications of nanofluids, concluding that nanofluids enhanced the heat transfer performance. Guo [10] studied the thermal performance of nanofluid with an artificial neural network, which was highlighted in particular. In a recent study, Souayeh et al. [11] numerically investigated the natural convective flow around two horizontally arranged spheres at a steady temperature utilizing three separate nanofluids. They found that the thermo-hydraulic performance of the nanofluids increased with the increase of Rayleigh number.

Because of the reports of considerably improved thermal characteristics, nanofluids have gained an immense focus in recent decades. Nanofluids' improved thermal conductivity and dynamic viscosity have widened the potential for enhanced thermal performance. Many experimentalists used their experimental data to provide the correlations of those properties for determining heat transfer rates. Einstein [12], Brinkman [13], and Batchelor [14] provided correlations for evaluating the absolute viscosity of the nanofluid, considering the solid-volume fraction of nanoparticles as one of the varying parameters. Besides, different correlations were given by many researchers to predict the thermal conduction coefficient of nanofluid. Xue [15] provided a novel thermal conductivity model of nanofluids based on average polarization and Maxwell theories. On the other hand, Jang and Choi [16], Prasher et al. [17], and Patel et al. [18] considered the effect of Brownian motion in devising the theoretical models of nanofluid thermal conductivity. Ren et al. [19] and Xie et al. [20] acknowledged the impact of interfacial nanolayers of liquid molecules in their thermal conductivity models. To suggest another correlation of thermal conductivity, Yang et al. [21] experimentally observed the heat transfer performance of nanofluids considering the effect of nanoparticle size and dispersed phase. A combined model of effective thermal conductivity, including the influences of Brownian motion, nanolayer, nanoparticle size, and surface chemistry, was proposed by Murshed et al. [22]. Among the recent studies, Xu et al. [23] investigated a novel method, called the improved steady-flow method, in determining the thermal conductivity of nanofluid and suggested that Al_2O_3-water nanofluid had great potential in the enhancement of thermal performance for a lower solid-volume fraction of nanofluid. Topal and Servantie [24] conducted a molecular dynamics simulation to calculate the thermal conductivity of nanofluids for various solid-volume fractions of nanofluids. They found enhanced thermal conductivity with a solid-volume fraction of 2%–3%. However, Raja and Sunil [25] estimated nanofluid thermal conductivity using different available models. They suggested that an extensive future investigation was necessary to determine the most reliable model for specific applications.

Despite the recent development, the above literature review confirms that a thorough investigation is still necessary to choose the best model of the thermo-physical properties of nanofluids. Thus, the current study compares the reliability of the available thermal conduction coefficient and absolute viscosity correlations of water-based Al_2O_3 nanofluid by estimating the free convection heat transfer characteristics. Firstly, the Prandtl numbers of the Al_2O_3-water nanofluid are analyzed from the evaluation of available models. Subsequently, a square-shaped differentially heated chamber filled with that nanofluid is considered to find the average Nusselt number employing different correlations of the thermal conduction coefficient and the absolute viscosity. These findings are compared to an experimental work to see which correlation produces the closest match.

2. Effective thermo-fluid properties of nanofluid

An essential task is accurately predicting the nanofluid's thermo-fluid properties to assess its thermal augmentation. A prevalent practice is gathering experimental data on nanofluid properties, mainly thermal conduction coefficient and absolute viscosity, and providing empirical correlations. The mixing theory calculates mass density, specific heat capacitance, and volumetric thermal expansion coefficient. These are the primary functions of base fluid properties, nanoparticle, and nanoparticle volume proportion. The thermo-fluid properties of water and Al_2O_3 listed in Table 1 are taken to compute the effective properties of Al_2O_3-water nanofluid.

The effective density, coefficient of volumetric thermal expansion, and specific heat capacity at fixed pressure of Al_2O_3-water nanofluid can be calculated following the mixing rule theory as given below,

$$\rho_{nf} = (1 - \varphi)\rho_{bf} + \varphi\rho_s, \tag{1}$$

Table 2
Some experimental works measuring the absolute viscosity of Al_2O_3-water nanofluid.

Researcher(s)	Nanoparticle Size (nm)	Measuring Technique	Remarks/Findings
Murshed et al. [22]	80	–	Derived theoretical model
Nguyen et al. [27]	36, 47	Piston-type viscometer	Proposed correlation
Ho et al. [28]	–	–	Proposed correlation
Azmi et al. [29]	–	–	Proposed correlation
Corcione [30]	25–200	–	Derived empirical model
Wang et al. [31]	28	1D steady state parallel plate	Discussed discrepancies associated with models
Putra et al. [32]	38	Rotating disk-type	Provided experimental data
Lee et al. [34]	–	Ultrasonic vibration.	Measured viscosity
Chandrasekar et al. [35]	43	Sonicator	Provided experimental data

$$(\rho\beta)_{nf} = (1-\varphi)(\rho\beta)_{bf} + \varphi(\rho\beta)_s, \tag{2}$$

$$\left(\rho C_p\right)_{nf} = (1-\varphi)\left(\rho C_p\right)_{bf} + \varphi\left(\rho C_p\right)_s, \tag{3}$$

where, the subscripts '*bf*', '*s*', and '*nf*' indicate the thermo-fluid properties of base fluid, nanoparticles, and nanofluid, respectively.

2.1. Effective dynamic viscosity

To estimate the effective absolute viscosity of nanofluid, Einstein [12], Brinkman [13], and Batchelor [14] developed the correlations for colloid dispersion, which many researchers frequently used. The calculated dynamic viscosity calculated from these correlations momentously underestimates the actual values. The degree of underestimation rises as the diameter of nanoparticles reduces and the concentration of nanoparticles increases [1]. Table 2 summarizes some experimental works measuring the absolute viscosity of water-Al_2O_3 nanofluid. The earlier model of viscosity, developed by Brinkman [13], can moderately evaluate the dynamic viscosity of any nanofluid for a specific range of nanoparticle solid-volume proportions ($0 \le \varphi \le 0.04$). The model can be written as follows,

$$\mu_{nf} = \frac{\mu_{bf}}{(1-\varphi)^{2.5}}. \tag{4}$$

After that, many researchers developed different effective dynamic viscosity models for different types of nanofluid. Nguyen et al. [27] formulated a dynamic viscosity model for Al_2O_3-water nanofluid ($0 \le \varphi \le 0.094$) as given below,

$$\mu_{nf} = 0.904e^{0.1483\varphi}\mu_{bf}. \tag{5}$$

Later, Ho et al. [28] conducted another experimental work for Al_2O_3-water nanofluid ($0 \le \varphi \le 0.04$) and provided an absolute viscosity model based on their experimental data as follows,

$$\mu_{nf} = \left(1 + 4.93\varphi + 222.4\varphi^2\right)\mu_{bf}. \tag{6}$$

Similarly, Azmi et al. [29] considered higher solid-volume fraction ($0 \le \varphi \le 0.10$) in their experiment and correlated the temperature-dependent dynamic viscosity by the following relation:

$$\mu_{nf} = \mu_{bf}(1+\varphi)^{11.3}\left(1 + \frac{t}{70}\right)^{-0.038}\left(1 + \frac{d_s}{170}\right)^{-0.061}, \tag{7}$$

where, t refers to the nanoparticles' temperature in °C and d_s is nanoparticles diameter in nm. Corcione [30] gathered experimental data on dynamic viscosity, which was a function of temperature, sizes, and solid-volume fraction of nanofluid, and provided a distinct correlation for a wide range of nanoparticle-volume fraction ($0.002 \le \varphi \le 0.09$). According to the data analysis of Corcione [30], the magnitude of dynamic viscosity was independent of temperature between 293 and 333 K. The correlation is written as,

$$\mu_{nf} = \frac{\mu_{bf}}{1 - 34.87\left(d_s/d_{bf}\right)^{-0.3}\varphi^{1.03}}, d_{bf} = 0.1\left(\frac{6M}{N\pi\rho_{bf}}\right)^{1/3}, \tag{8}$$

where, M and N indicate the molar mass of the base fluid and Avogadro number, respectively, and d_{bf} is the equivalent diameter of the base fluid molecule.

2.2. Effective thermal conductivity

Experimental works measuring the thermal conduction coefficient of Al_2O_3-water nanofluid are also listed in Table 3. Maxwell [36] gave an empirical model to find the thermal conduction coefficient of nanofluids ($0 \le \varphi \le 0.04$) at room temperature:

Table 3
Some experimental works measuring the thermal conduction coefficient of Al_2O_3-water nanofluid.

Researcher(s)	Nanoparticle Size (nm)	Measuring Method	Remarks/Findings
Choi and Eastman [1]	38.4	Hot-wire transient	Measured conductivity
Murshed et al. [22]	80	Hot-wire transient	Derived theoretical model
Ho et al. [28]	–	–	Proposed correlation
Azmi et al. [29]	–	–	Proposed correlation
Corcione [30]	10–150	–	Derived empirical model
Li and Peterson [33]	36	Hot-wire transient	Proposed correlation
Lee et al. [34]	–	Ultrasonic vibration	Measured conductivity
Chandrasekar et al. [35]	43	Sonicator	Measured conductivity
Das et al. [37]	28.6	Oscillation	Measured conductivity
Chon et al. [38]	47	Hot-wire transient	Derived empirical correlation
Zang et al. [39]	–	Transient SWH	Measured conductivity
Moldoveanu et al. [40]	43	Transient	Proposed correlation
Kumar et al. [41]	–	KD2 Pro digital recorder	Measured conductivity

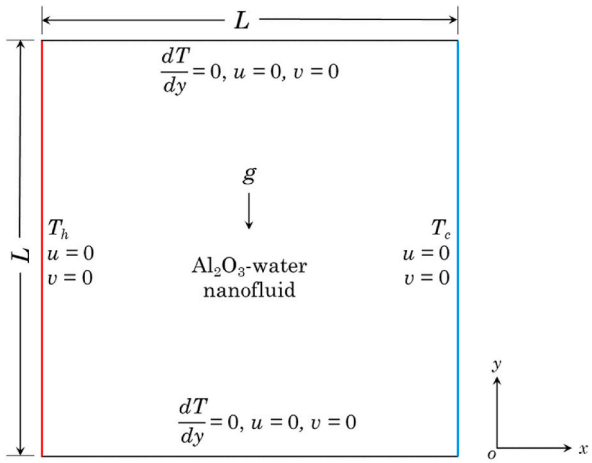

Fig. 1. Computational domain of the present investigation.

$$k_{nf} = \frac{k_s + 2k_{bf} - 2\varphi\left(k_{bf} - k_s\right)}{k_s + 2k_{bf} + \varphi\left(k_{bf} - k_s\right)} k_{bf}. \tag{9}$$

This model tends to fail drastically when the suspension temperature is above 20°C. Li and Peterson [33] experimentally showed the limitation of Maxwell's model and derived a temperature-dependent equation for estimating the thermal conduction coefficient of nanofluids as,

$$k_{nf} = (0.764\varphi + 0.0187t - 0.462)k_{bf} + k_{bf}. \tag{10}$$

Another two thermal conductivity models of water-Al_2O_3 nanofluid were given by Ho et al. [28] and Azmi et al. [29], where they considered the nanoparticle-volume proportion within $0 \le \varphi \le 0.04$ and $0 \le \varphi \le 0.10$, respectively. Those models are given below:

$$k_{nf} = \left(1 + 2.944\varphi + 19.672\varphi^2\right)k_{bf}, \tag{11}$$

$$k_{nf} = 0.8938(1+\varphi)^{1.37}\left(1 + \frac{t}{70}\right)^{0.2777}\left(1 + \frac{d_s}{170}\right)^{-0.0336}\left(\frac{\alpha_s}{\alpha_{bf}}\right)^{0.01737} k_{bf}, \tag{12}$$

where, α denotes thermal diffusivity. Corcione [30] also provided a model of thermal conductivity, which can be given as follows,

$$k_{nf} = k_{bf}\left[1 + 4.4Re^{0.4}Pr^{0.66}\left(\frac{T}{T_{fr}}\right)^{10}\left(\frac{k_s}{k_{bf}}\right)^{0.03}\varphi^{0.66}\right], Re = \frac{2\rho_{bf}k_b T}{\pi\mu_{bf}^2 d_s}, Pr_{bf} = \frac{\mu_{bf}C_{p,bf}}{k_{bf}}, \tag{13}$$

where, Pr_{bf} and T_{fr} denote the Prandtl number and the freezing point temperature of the base fluid (water), Re indicates the Brownian-motion Reynolds number, k_b is Boltzmann's constant, and T is the nanofluid's temperature in K.

Table 4
List of auxiliary conditions imposed on the square cavity.

Boundary wall	Velocity Vector	Temperature State
Left wall	$\boldsymbol{U} = 0$	$\Theta = 1$
Right wall		$\Theta = 0$
Top and bottom walls		$\partial\Theta/\partial Y = 0$

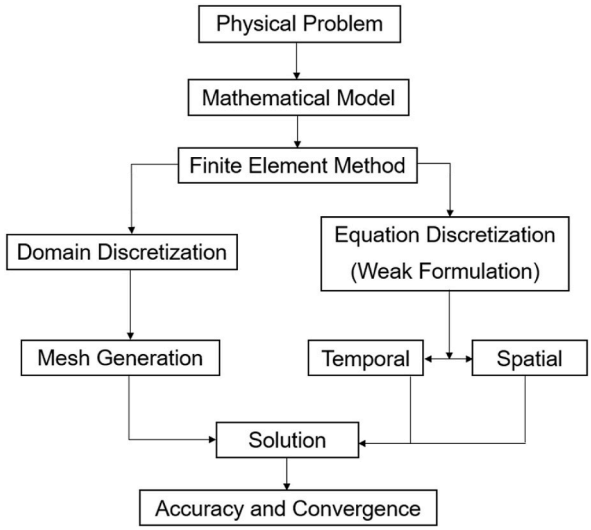

Fig. 2. Flow diagram of the step-by-step solution algorithm using the finite element method.

3. Test problem and numerical simulation

A differentially heated chamber of equal length L filled with water-Al_2O_3 nanofluid, as shown in Fig. 1, is selected as a test configuration. The nanofluid is supposed to be incompressible, and Newtonian, and its flow regime is steady, two-dimensional, and laminar. The chamber's left and right solid surfaces are fixed at differential temperature ($T_h > T_c$), while the horizontal top and bottom boundaries are kept adiabatic.

A summary of the dimensionless auxiliary conditions applied to the square cavity has been presented in Table 4. The nanoparticle-volume fraction of water-Al_2O_3 nanofluid is changed inside the chamber between 0 and 4%. The effective density, coefficient of volumetric thermal expansion, and heat capacitance of Al_2O_3-water nanofluid are calculated from (1) to (3), respectively. The correlations shown in (4) to (13) are utilized in calculating the nanofluid's viscosity and thermal conduction coefficient. The Rayleigh number (Ra) is changed from 10^3 to 10^9 to compare the system's thermal and hydrodynamic performances under different nanofluid models. The governing models used in the test problem are continuity, momentum, and thermal energy equations. The dimensionless forms of those equations are presented as,

$$\nabla \cdot \boldsymbol{U} = 0, \tag{14}$$

$$(\boldsymbol{U} \cdot \nabla)\boldsymbol{U} = \nabla\left[- P\mathbf{I} + \frac{\nu_{nf}}{\nu_{bf}} Pr_{bf}\left\{\nabla \boldsymbol{U} + (\nabla \boldsymbol{U})^T\right\}\right] + \boldsymbol{F}, \tag{15}$$

$$\boldsymbol{U} \cdot \nabla\Theta = \frac{\alpha_{nf}}{\alpha_{bf}} \nabla^2\Theta, \tag{16}$$

where, $\boldsymbol{U}$, P, and Θ are the non-dimensional nanofluid's velocity vector, pressure, and temperature, respectively. The body force vector is expressed as $\boldsymbol{F} = (0, \beta_{nf} Ra Pr_{bf} \Theta/\beta_{bf})$. In those governing equations, the crucial controlling parameter (Ra) is introduced in terms of base fluid's properties, which is expressed as (17):

$$Ra = \frac{g\beta_{bf}(T_h - T_c)L^3}{\nu_{bf}\alpha_{bf}}, \tag{17}$$

where, ν and g are kinematic viscosity, and gravitational acceleration, respectively. The average Nusselt number is calculated at the hot isothermal left surface to express the system's thermal performance. The following formula defines it as,

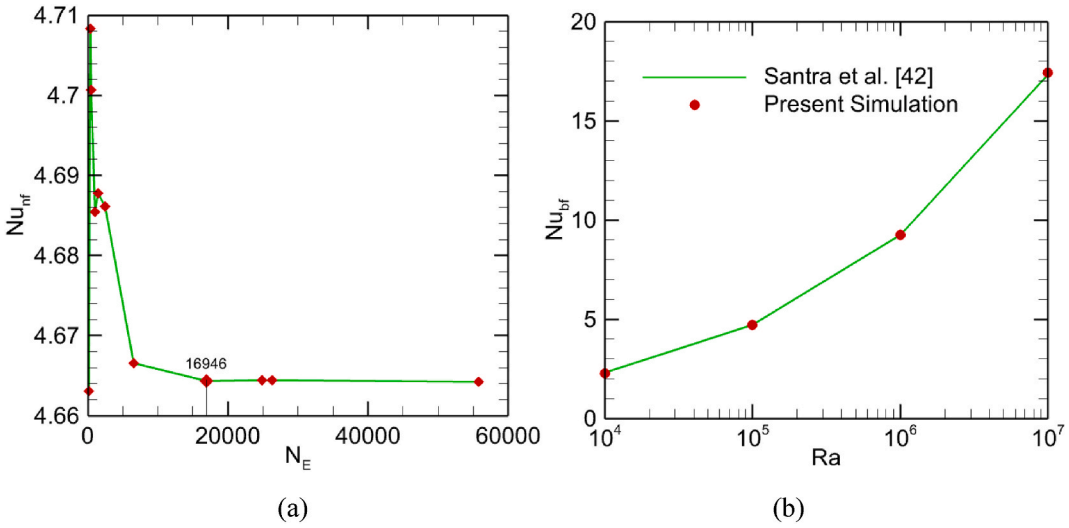

Fig. 3. (a) Grid independence test of the benchmark problem for $Ra = 10^5$ and $\varphi = 0.01$, and (b) validation of the present model with the numerical simulation of Santra et al. [42] in terms Nu_{bf} for base fluid (water) with $Pr = 7.02$ (color online). (For interpretation of the references to color in this figure legend, the reader is referred to the Web version of this article.)

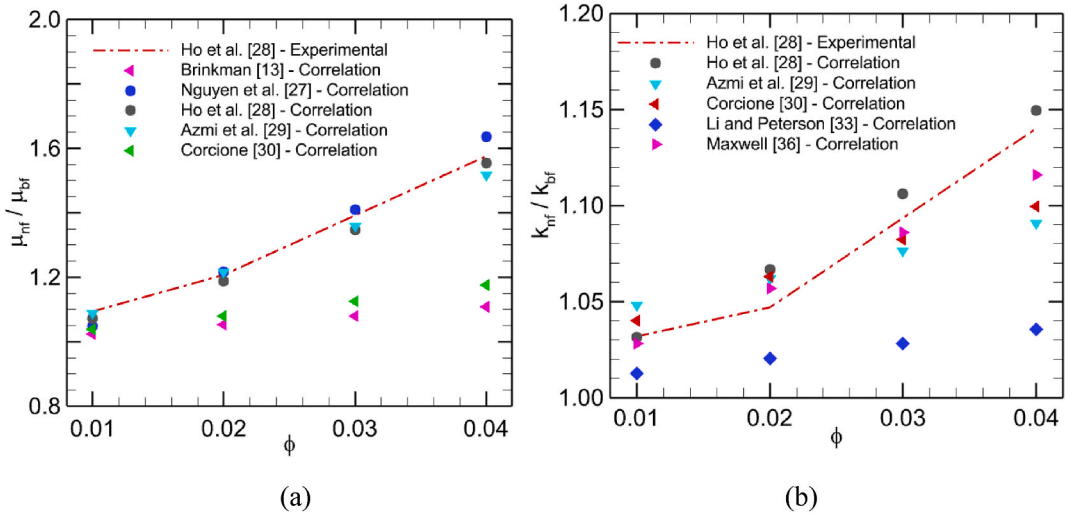

Fig. 4. Discrepancy of (a) the effective normalized absolute viscosity and (b) the effective normalized thermal conduction coefficient of water-Al_2O_3 nanofluid with the variation of φ (color online). (For interpretation of the references to color in this figure legend, the reader is referred to the Web version of this article.)

$$Nu = -\frac{k_{nf}}{k_{bf}} \int_0^1 \frac{\partial \Theta}{\partial X} dY, \tag{18}$$

where, X and Y are dimensionless Cartesian frameworks.

To solve the governing equations (14)–(16) alongside the auxiliary conditions, the Galerkin finite element method-based commercial software program "COMSOL Multiphysics 6.1" is used. First, the computational domain has been discretized into triangular mesh elements, and the governing equations are applied to the individual element. Then, the solution of the nonlinear governing algebraic finite element equations is obtained using the Newton-Raphson iteration procedure. When the relative percentage of error goes below a certain threshold, the solution procedure is assumed to be completed. The error limit follows this terminating criterion: $\gamma^{m+1} - \gamma^m < 10^{-5}$, where γ and m are the general independent variable and number of iterations, respectively. The step-by-step solution procedure is depicted in Fig. 2. Before performing parametric simulation, an optimum mesh of 16,946 elements is selected via an extensive test of grid refinement, as illustrated in Fig. 3(a). The present model is validated against a computational study by Santra

Table 5
Combinations of different existing models of the effective absolute viscosity and the thermal conduction coefficient of nanofluid.

Model ID	Viscosity Model	Thermal Conductivity Model	Symbol
NM	Nguyen et al. [27]	Maxwell [36]	
NH	Nguyen et al. [27]	Ho et al. [28]	
NA	Nguyen et al. [27]	Azmi et al. [29]	
AM	Azmi et al. [29]	Maxwell [36]	
AH	Azmi et al. [29]	Ho et al. [28]	
AA	Azmi et al. [29]	Azmi et al. [29]	
HM	Ho et al. [28]	Maxwell [36]	
HH	Ho et al. [28]	Ho et al. [28]	
HA	Ho et al. [28]	Azmi et al. [29]	
CC	Corcione [30]	Corcione [30]	
HH_exp	Ho et al. [28] experimental	Ho et al. [28] experimental	

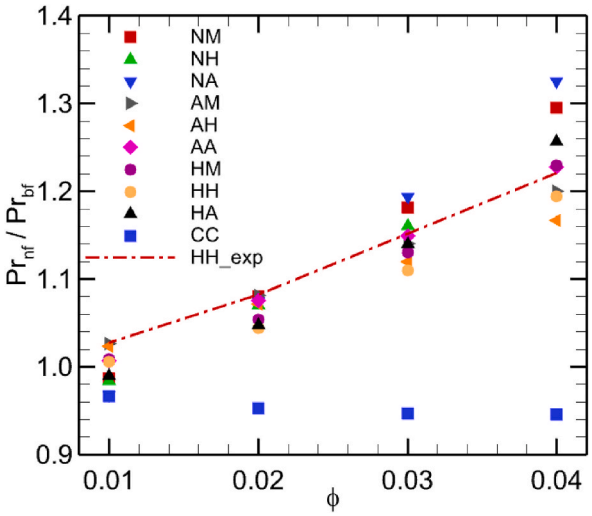

Fig. 5. Comparison of normalized Prandtl numbers of Al_2O_3-water nanofluid with the variation of φ for different combinations of models as listed in Table 5 (color online). (For interpretation of the references to color in this figure legend, the reader is referred to the Web version of this article.)

et al. [42], as shown in Fig. 3(b), to support the justification of the computational strategy and numerical accuracy. The comparison of the average Nusselt number (calculated using (18)) reveals that the current model and the computations of the numerical scheme are consistent and accurate, thus providing enough confidence for further computational outcomes.

4. Results and discussion

The effective dynamic viscosity of nanofluid is calculated using the correlations (4) to (8), ranging the solid-volume proportion of nanoparticles from 0 to 4%. The variation of the normalized dynamic viscosity is illustrated in Fig. 4(a). It can be said that Brinkman [13] and Corcione [30] models are not predicting well enough compared to the experimental results of Ho et al. [28]. It is important to note that their experimental work [28] is considered here since their evaluated geometrical configuration (square cavity), boundary conditions (differentially heated), and thermal transport mode (free convection) are identical to the current test problem.

Similarly, the effective thermal conduction coefficient of Al_2O_3-water nanofluid is computed using the correlations (9) to (13) within similar relative proportions of nanoparticle volume proportion. The results from various models are presented in Fig. 4(b). It is observed that Li and Peterson's [33] model shows a poor estimation in comparison with the experimental measurements of Ho et al.

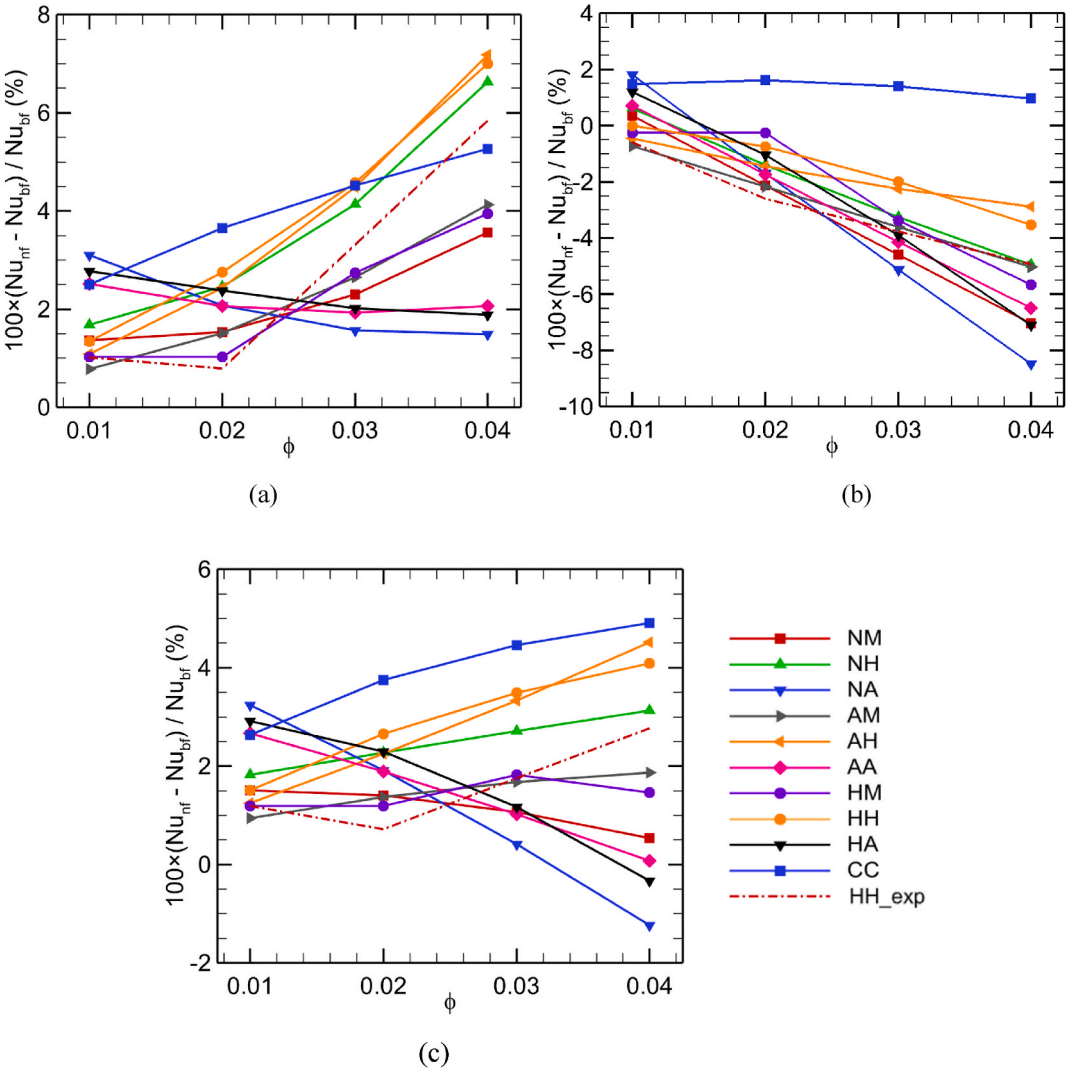

Fig. 6. Comparison of % change of *Nu* of Al_2O_3-water nanofluid with the variation of φ for different combinations of models as listed in Table 5 at (a) $Ra = 10^3$, (b) $Ra = 10^6$, and (c) $Ra = 10^9$ (color online). (For interpretation of the references to color in this figure legend, the reader is referred to the Web version of this article.)

[28].

Since Brinkman's [13] dynamic viscosity model and Li and Peterson's [33] thermal conduction coefficient model differ significantly from the experimental data, further investigation excludes these two models. Ten combinations of different existing models, along with the experimental results of Ho et al. [28] on thermal conduction coefficient and dynamic viscosity listed in Table 5, are taken for further analysis of the performance of water-Al_2O_3 nanofluid. For comparison, the solid-volume proportion is chosen within 0–4%.

The Prandtl number of nanofluid is ($Pr_{nf} = \nu_{nf}/\alpha_{nf}$, where ν is kinematic viscosity) evaluated using the properties listed in Table 1. The normalized Prandtl numbers (Pr_{nf}/Pr_{bf}) for all eleven combinations are displayed in Fig. 5. The values of Pr_{nf}/Pr_{bf} calculated from the experimental results of Ho et al. [28] are also shown here. It can be observed that the trend of variation of the Prandtl number with the variation of φ is similar for all combinations except the Corcione [30] models. It might be due to including all the uncertainties of different experimental works in a single model since he took a wide range of data from his literature review.

For all combinations, the percentage change of *Nu* is plotted in Fig. 6 for solid-volume fraction 1–4% at three different Rayleigh numbers (10^3, 10^6, and 10^9). From Fig. 6(a), it can be seen that the percentage change of *Nu* is almost greater than unity for the entire range of φ, which contemplates the augmentation of heat transfer performance at $Ra = 10^3$. For $Ra = 10^6$, as shown in Fig. 6(b), heat transfer performance is enhanced only for lower solid-volume proportion ($\varphi = 0.01$), and for higher values ($\varphi > 0.01$), it deteriorates. When both *Ra* and solid-volume fraction increase, two opposite effects occur: higher *Ra* increases the buoyancy effect to increase the heat transfer, and higher solid-volume fraction means higher viscosity, which ultimately reduces the impact of *Ra*. For a moderate

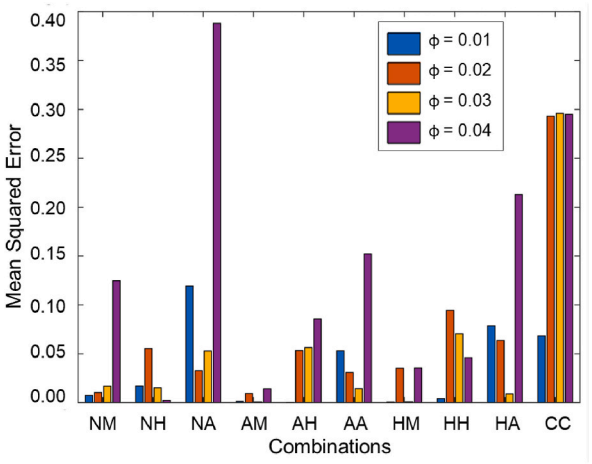

Fig. 7. Variation of mean squared error of *Nu* with respect to the experimental results of Ho et al. [28] within $10^3 \leq Ra \leq 10^9$.

Table 6
Mean squared error of *Nu* with respect to the experimental results of Ho et al. [28] within $10^3 \leq Ra \leq 10^9$.

Combination	Solid-volume fraction (φ)			
	0.01	0.02	0.03	0.04
NM	0.00734	0.01030	0.01679	0.12472
NH	0.01696	0.05541	0.01515	**0.00224**
NA	0.11931	0.03258	0.05275	0.38810
AM	0.00124	**0.00937**	**0.00063**	0.01417
AH	**0.00018**	0.05319	0.05634	0.08565
AA	0.05292	0.03088	0.01430	0.15208
HM	0.00057	0.03530	0.00074	0.03555
HH	0.00417	0.09438	0.07057	0.04603
HA	0.07848	0.06353	0.00896	0.21287
CC	0.06821	0.29319	0.29596	0.29504

value of Ra ($=10^6$), the effect of increasing viscosity dominates over the effect of buoyancy, for which overall heat transfer performance deteriorates. However, superior heat transfer performance is obtained at $Ra = 10^9$, as shown in Fig. 6(c), except for slight deterioration at $\varphi = 0.04$ by a few combinations. At this value of Ra, severe mixing of the nanofluid occurs due to higher buoyancy-induced fluid motion, and this phenomenon surpassed the negative effect of the increasing viscosity of nanofluids at higher solid-volume fractions. The next task is to find the closeness of the results evaluated by the nanofluid models with the experimental data to get into the final selection.

The mean squared error (MSE) of *Nu* with the experimental measurements of Ho et al. [28] for all combinations of models are illustrated in Fig. 7. It can be summarized from the figure that among all the varieties, NM, NA, AA, HH, HA, CC show very poor closeness for the entire range of solid-volume fraction. Besides, the quantitative data of the mean squared errors are presented in Table 6 to select the best combinations. Observing the MSE values confirmed that for solid-volume proportion $\varphi = 0.01$, the AH combination gives a closer result to the experimental work. However, for solid-volume proportions in the range of 0.02–0.03, it can be emphasized that the combination of AM outperforms other combinations. Finally, using the NH combination to estimate the nanofluid's thermal conduction coefficient and absolute viscosity is better at $\varphi = 0.04$.

Further, the variation of percentage change of *Nu* with the interpretation of *Ra* is plotted, as shown in Fig. 8(a)-(c), to compare how the best-selected combinations predict the heat transfer performance. It is apparent for all three varieties that the heat transfer rate increases with increasing solid-volume proportions at a lower Rayleigh number. In this case, the effect of enhanced thermal conduction coefficient is dominant compared to the impact of enhanced viscosity. However, a worsened heat transfer performance is observed for a wide range of Rayleigh numbers ($10^4 \leq Ra \leq 10^8$). The reduction of thermal performance is prominent for higher solid-volume fractions ($\varphi \geq 0.02$) because of the impediment in natural convection by the nanoparticles, and it is justified by the finding of Nnanna [43]. Finally, the deterioration continues until turbulence ($Ra > 10^8$) is introduced in the flow regime.

Now, the closeness of the models with the experimental data can be visualized in those figures. For $\varphi = 0.01$, the AH and AM models are relatively close to the experimental data according to Fig. 8(a) and (b). However, the AH model is more closely fitted than the AM model. Then, in the case of $\varphi = 0.02$ and 0.03, the AM model shows the best fit compared to any other models, as seen in Fig. 8(b). Finally, according to Fig. 8(c), the NH model can be chosen to get the best result for $\varphi = 0.04$.

In the case of statistical analysis, Corcione's proposed models [30] can be considered since he gathered extensive data from the literature and presented the correlations. Though the variation trend of *Nu* is similar to those of AH, AM, and NH models, as shown in

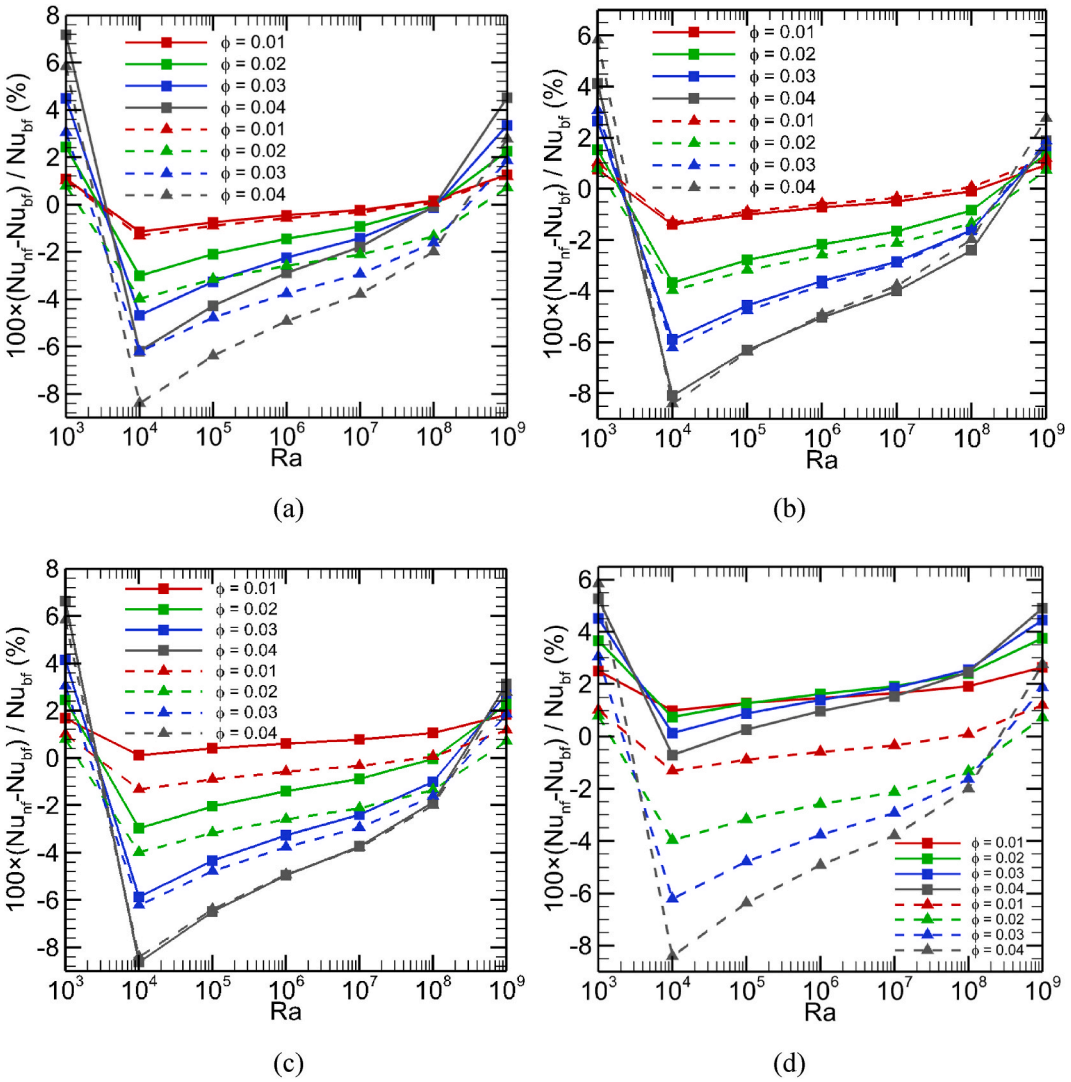

Fig. 8. Variation of percentage change of *Nu* of water-based Al_2O_3 nanofluid against *Ra* for different φ during the combination of (a) AH, (b) AM, (c) NH, and (d) CC (color online). Solid and dashed lines indicate correlational and experimental data, respectively. (For interpretation of the references to color in this figure legend, the reader is referred to the Web version of this article.)

Fig. 8(d), it contemplates the enhancement of heat transfer for almost the entire range of *Ra*. This result is contradictory to the findings of the experimental work of Ho et al. [28].

5. Conclusion

This paper comparatively studies and presents different available effective absolute viscosity and thermal conduction coefficient models. As heat transfer augmentation in various devices is highly desired, making a linkage between simulation and experimental work with the closest prediction of thermo-physical properties is compulsory.

A benchmark problem of the differentially heated cavity is selected to analyze the Al_2O_3-water nanofluid's natural convection. Ten combinations of the absolute viscosity and the thermal conduction coefficient models of the nanofluid are thoroughly investigated since these properties are vital functions of the solid-volume fraction of nanoparticles, nanoparticle size, temperature, etc. The coefficient of heat transfer also strongly depends on the absolute viscosity and thermal conduction coefficient. The rest of the required properties are estimated by using the general mixing theory. The findings can be summarized as follows:

i. According to the experimental and simulation data agreement, AH, AM, and NH combinations seemed the most reliable. However, AH can be suggested for lower nanoparticle concentration ($\varphi = 0.01$), AM for moderate concentration ($0.01 < \varphi < 0.04$), and NH for higher value of the solid-volume proportion ($\varphi = 0.04$).

ii. To calculate individual properties of nanofluid, viscosity models of Nguyen et al. [27] and Azmi et al. [29] and conductivity models of Ho et al. [28] and Maxwell [36] can be used with minimum uncertainty.
iii. Moreover, nanofluids are often considered as single-phase fluids in simulation-based works. This assumption limits the effect of particle size, stability, and other physical mechanisms happening inside the nanofluid, such as thermophoresis, dispersion, clustering, Brownian motion, etc. Besides, using a complex empirical correlation associated with much detailed physics is often considered impractical in many engineering applications. Therefore, identifying the most effective correlations with a trade-off between the accuracy of the results and the computational complexity is vital. In this regard, the selected models show good concurrency.
iv. The nanofluid properties and the heat transfer mechanism still require a lot of detailed computational and experimental investigations to make a more generalized way of solving such thermal system problems.

Data availability statement

Data will be made available on request.

CRediT authorship contribution statement

Tahmidul Haque Ruvo: Writing – review & editing, Writing – original draft, Visualization, Validation, Investigation, Formal analysis, Conceptualization. **Md. Shahneoug Shuvo:** Writing – review & editing, Writing – original draft, Methodology, Investigation, Data curation. **Sumon Saha:** Writing – review & editing, Writing – original draft, Supervision, Software, Formal analysis, Data curation, Conceptualization.

Declaration of competing interest

The authors declare that they have no known competing financial interests or personal relationships that could have appeared to influence the work reported in this paper.

Acknowledgments

We thank CFDHT Research Group and Basic Research Grant of BUET [grant # 4747(45), SL#09, date: April 13, 2022] for their invaluable assistance during our research.

References

[1] S.S.U. Choi, J.A. Eastman, Enhancing thermal conductivity of fluids with nanoparticles, ASME Publ 66 (1995) 99–105.
[2] R. Ben Mansour, N. Galanis, C.T. Nguyen, Effect of uncertainties in physical properties on forced convection heat transfer with nanofluids, Appl. Therm. Eng. 27 (2007) 240–249.
[3] B. Souayeh, K.A. Abro, H. Alfannakh, M.A. Nuwairan, A. Yasin, Application of Fourier sine transform to carbon nanotubes suspended in ethylene glycol for the enhancement of heat transfer, Energies 15 (2022) 1200.
[4] B. Souayeh, K.A. Abro, A. Siyal, N. Hdhiri, F. Hammami, M. Al Shaeli, N. Alnaim, S.S.K. Raju, M.W. Alam, Role of copper and alumina for heat transfer in hybrid nanofluid by using Fourier sine transform, Sci. Rep. (2022) 1–11.
[5] S. Kakaç, A. Pramuanjaroenkij, Review of convective heat transfer enhancement with nanofluids, Int. J. Heat Mass Tran. 52 (2009) 3187–3196.
[6] A. Kasaeian, R.D. Azarian, O. Mahian, L. Kolsi, A.J. Chamkha, S. Wongwises, I. Pop, Nanofluid flow and heat transfer in porous media: a review of the latest developments, Int. J. Heat Mass Tran. 107 (2017) 778–791.
[7] R.V. Pinto, F.A.S. Fiorelli, Review of the mechanisms responsible for heat transfer enhancement using nanofluids, Appl. Therm. Eng. 108 (2016) 720–739.
[8] A.M. Hussein, K.V. Sharma, R.A. Bakar, K. Kadirgama, A review of forced convection heat transfer enhancement and hydrodynamic characteristics of a nanofluid, Renew. Sustain. Energy Rev. 29 (2014) 734–743.
[9] I.A. Ismail, M.Z. Yusoff, F.B. Ismail, P. Gunnasegaran, Heat transfer enhancement with nanofluids: a review on recent applications and experiments, AIP Conf. Proc. 2035 (2018).
[10] Z. Guo, A review on heat transfer enhancement with nanofluids, J. Enhanc. Heat Transf. 27 (2020) 1–70.
[11] B. Souayeh, F. Hammami, N. Hdhiri, M.W. Alam, E. Yasin, A. Abuzir, Simulation of natural convective heat transfer and entropy generation of nanoparticles around two spheres in horizontal arrangement, Alex. Eng. J. (2021) 2583–2605.
[12] A. Einstein, A new determination of molecular dimensions, Ann. Phys. 19 (1906) 289–306.
[13] H.C. Brinkman, The viscosity of concentrated suspensions and solutions, J. Chem. Phys. 20 (1952) 571.
[14] G.K. Batchelor, The effect of Brownian motion on the bulk stress in a suspension of spherical particles, Exercer 83 (2016) 40–41.
[15] Q. Xue, Model for effective thermal conductivity of nanofluids, Phys. Lett. 307 (2003) 313–317.
[16] S.P. Jang, S.U.S. Choi, Role of Brownian motion in the enhanced thermal conductivity of nanofluids, Appl. Phys. Lett. 84 (2004) 4316–4318.
[17] R. Prasher, P. Bhattacharya, P.E. Phelan, Thermal conductivity of nanoscale colloidal solutions (nanofluids), Phys. Rev. Lett. 94 (2005) 3–6.
[18] H.E. Patel, T. Sundararajan, T. Pradeep, A. Dasgupta, N. Dasgupta, S.K. Das, A micro-convection model for thermal conductivity of nanofluids, Pramana - J. Phys. 65 (2005) 863.
[19] Y. Ren, H. Xie, A. Cai, Effective thermal conductivity of nanofluids containing spherical nanoparticles, J. Phys. D Appl. Phys. 38 (2005) 3958–3961.
[20] H. Xie, M. Fujii, X. Zhang, Effect of interfacial nanolayer on the effective thermal conductivity of nanoparticle-fluid mixture, Int. J. Heat Mass Tran. 48 (2005) 2926–2932.
[21] Y. Yang, Z.G. Zhang, E.A. Grulke, W.B. Anderson, G. Wu, Heat transfer properties of nanoparticle-in-fluid dispersions (nanofluids) in laminar flow, Int. J. Heat Mass Tran. 48 (2005) 1107–1116.
[22] S.M.S. Murshed, K.C. Leong, C. Yang, A combined model for the effective thermal conductivity of nanofluids, Appl. Therm. Eng. 29 (2009) 2477–2483.
[23] G. Xu, J. Fu, B. Dong, Y. Quan, G. Song, A novel method to measure thermal conductivity of nanofluids, Int. J. Heat Mass Tran. 130 (2019) 978–988.
[24] I. Topal, J. Servantie, Molecular dynamics study of the thermal conductivity in nanofluids, Chem. Phys. 516 (2019) 147–151.

[25] R.A.A. Raja, J. Sunil, R. Maheswaran, Estimation of thermo-physical properties of nanofluids using theoretical correlations, Int. J. Appl. Eng. Res. 13 (2018) 7950–7953.
[26] A.A. Minea, A review on the thermophysical properties of water-based nanofluids and their hybrids, Ann. "Dunarea Jos" Univ. Galati Fascicle IX. Metall. Mater. Sci. 34 (2016) 35–47.
[27] C.T. Nguyen, F. Desgranges, N. Galanis, G. Roy, T. Maré, S. Boucher, H. Angue Mintsa, Viscosity data for Al_2O_3-water nanofluid-hysteresis: is heat transfer enhancement using nanofluids reliable? Int. J. Therm. Sci. 47 (2008) 103–111.
[28] C.J. Ho, W.K. Liu, Y.S. Chang, C.C. Lin, Natural convection heat transfer of alumina-water nanofluid in vertical square enclosures: an experimental study, Int. J. Therm. Sci. 49 (2010) 1345–1353.
[29] W.H. Azmi, K.V. Sharma, R. Mamat, S. Anuar, Nanofluid properties for forced convection heat, J. Mech. Eng. Sci. 4 (2013) 397–408.
[30] M. Corcione, Empirical correlating equations for predicting the effective thermal conductivity and dynamic viscosity of nanofluids, Energy Convers. Manag. 52 (2011) 789–793.
[31] X. Xu, S.U.S. Choi, X. Wang, Thermal conductivity of nanoparticle - fluid mixture, J. Thermophys. Heat Tran. 13 (1999) 474–480.
[32] N. Putra, W. Roetzel, S.K. Das, Natural convection of nanofluids, Heat Mass Tran. 39 (2003) 775–784.
[33] C.H. Li, G.P. Peterson, Experimental investigation of temperature and volume fraction variations on the effective thermal conductivity of nanoparticle suspensions (nanofluids), J. Appl. Phys. 99 (2006).
[34] J.H. Lee, K.S. Hwang, S.P. Jang, B.H. Lee, J.H. Kim, S.U.S. Choi, C.J. Choi, Effective viscosities and thermal conductivities of aqueous nanofluids containing low volume concentrations of Al_2O_3 nanoparticles, Int. J. Heat Mass Tran. 51 (2008) 2651–2656.
[35] M. Chandrasekar, S. Suresh, A. Chandra Bose, Experimental investigations and theoretical determination of thermal conductivity and viscosity of Al2O3/water nanofluid, Exp. Therm. Fluid Sci. 34 (2010) 210–216.
[36] J.C. Maxwell, A Treatise on Electricity and Magnetism, third ed., Oxford University Press, London, 1873.
[37] S.K. Das, N. Putra, P. Thiesen, W. Roetzel, Temperature dependence of thermal conductivity enhancement for nanofluids, J. Heat Tran. 125 (2003) 567–574.
[38] C.H. Chon, K.D. Kihm, S.P. Lee, S.U.S. Choi, Empirical correlation finding the role of temperature and particle size for nanofluid (Al_2O_3) thermal conductivity enhancement, Appl. Phys. Lett. 87 (2005) 1–3.
[39] X. Zhang, H. Gu, M. Fujii, Experimental study on the effective thermal conductivity and thermal diffusivity of nanofluids, Int. J. Thermophys. 27 (2006) 569–580.
[40] G.M. Moldoveanu, G. Huminic, A.A. Minea, A. Huminic, Experimental study on thermal conductivity of stabilized Al_2O_3 and SiO_2 nanofluids and their hybrid, Int. J. Heat Mass Tran. 127 (2018) 450–457.
[41] N. Kumar, S.S. Sonawane, S.H. Sonawane, Experimental study of thermal conductivity, heat transfer and friction factor of Al_2O_3 based nano fl uid, Int. Commun. Heat Mass Tran. 90 (2018) 1–10.
[42] A.K. Santra, S. Sen, N. Chakraborty, Study of heat transfer augmentation in a differentially heated square cavity using copper-water nanofluid, Int. J. Therm. Sci. 47 (2008) 1113–1122.
[43] A.G.A. Nnanna, Experimental model of temperature-driven nanofluid, J. Heat Tran. 129 (2007) 697–704.

Nomenclature

C_p: Specific heat ($Jkg^{-1}K^{-1}$)
d: diameter (m)
$\boldsymbol{F}$: Dimensionless body force vector
g: Gravitational acceleration (ms^{-2})
$\boldsymbol{I}$: Identity vector
k: Thermal conductivity ($Wm^{-1}K^{-1}$)
k_b: Boltzmann constant (1.38066 JK^{-1})
L: Length of the cavity (m)
M: Molar mass of base fluid
N: Avogadro number
N_E: Number of mesh elements
Nu: Average Nusselt number
P: Dimensionless pressure
Pr: Prandtl number
Ra: Rayleigh number
Re: Reynolds number
t: temperature of nanofluid (°C)
T: Temperature of nanofluid (K)
$\boldsymbol{U}$: Dimensionless velocity vector (ms^{-1})
X, Y: Dimensionless Cartesian coordinates

Greek Symbols

α: Thermal diffusivity (m^2s^{-1})
β: Thermal expansion coefficient (K^{-1})
Θ: Dimensionless temperature
μ: Dynamic viscosity (Pa.s)
ν: Kinematic viscosity (m^2s^{-1})
ρ: density (kgm^{-3})
φ: Solid-volume fraction of nanoparticles

Subscripts

bf: Base fluid
c: Cold wall
fr: Freezing point of base fluid
h: Hot wall
nf: Nanofluid
s: nanoparticles